Asian Journal of Green Chemistry 8 (2024) 382-396

Asian Journal of Green Chemistry

Original Research Article View Article Online | View Journal

Synthesis and Characterization of Acrylamide-Based Graft Poly(Acrylic Acid) Hydrogel Nanocomposite for Methylene Blue Dye Removal and Investigation Isotherm Models

Aseel M. Aljeboree, Ola Hamad Salah, Manal Morad Karim, Salima B. Alsaadi, Mohammed Abed Jawad, Ayad F. Alkaim*

Al-Farahidi University, Pharmacy College, Department of Pharmaceutics, Baghdad, Iraq

ARTICLE INFORMATION

Submitted: 2024-03-05
Revised: 2024-05-08
Accepted: 2024-05-09
Manuscript ID: AJGC-2405-1501
Checked for Plagiarism: Yes
Language Editor Checked: Yes

DOI: 10.48309/AJGC.2024.455843.1501

KEYWORDS

Adsorption
Methylene blue
Isotherm
Hydrogel
Acrylic acid

ABSTRACT

In this study, acrylamide based graft poly (acrylic acid) hydrogel (AM-g-P(AC)) and its nanocomposite with CdS nanoparticles AM-g-P(AC)/CdS were produced by the free radical method and utilized for methylene blue (MB) dye removal from aqueous solution. The characterization and properties of the adsorbents were studied utilizing FESEM, FTIR, TGA, and XRD analyses, and the results showed that CdS NPs were successfully distributed in the hydrogel structure. CdS NPs were loaded into the hydrogel system and the best adsorption capacity of MB dye was determined at 0.05 g of Cds NPs. Also, the effect of equilibrium time, initial concentration, temperature, and initial pH on the adsorption capacity of MB dye was studied. Behavior of the equilibrium investigation of the adsorption method show that the equilibrium result determined are in the best agreement with the Freundlich isotherm model and the multilayer surfaces play an effective role in the adsorption method. The best multilayer adsorption efficiency (q_{max}) determined utilizing isotherm Freundlich model for AM-g-P(AC)/CdS. The maximum adsorption capacity (Qe mg/g) determined for CMC-g-P(AAm) and AM-g-P(AC)/CdS were determined as 534.45 mg/g and 467.67 mg/g, respectively. The biological compound activity results were observed before and after the process of loading CdS NPs on it against the types of bacteria tested (*Staphylococcus epidermidi* and *Staphylococcus aureus*) and (*E. coli* and *Klebsiella spp.)*.

Corresponding authors, email: alkaimayad@gmail.com (A.F. Alkaim).
Tel.: 9647801324986.

Graphical Abstract

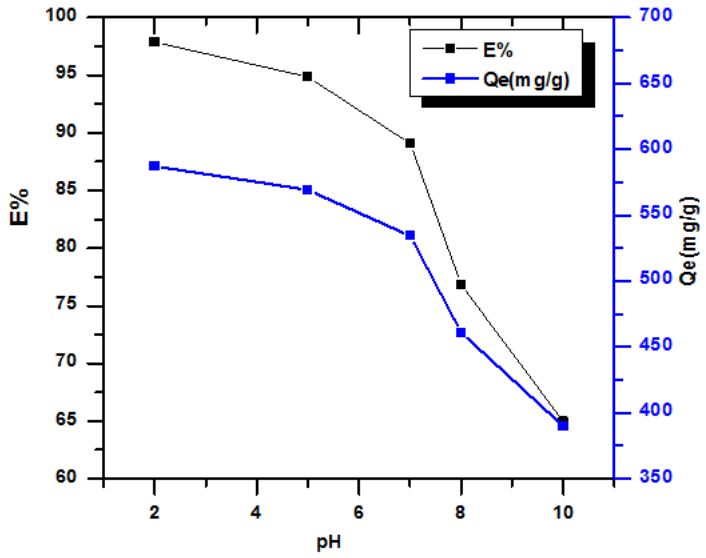

Introduction

Textile dyes are widely used in many industries, such as the dyeing, tanning, papermaking, and pharmaceutical industries, due to the wide use of these dyes, the low cost of their production, their colors, their resistance to many environmental influences, and the ease of application [1]. Various approaches have been developed to eliminate dyes from industrial waste water which contain electrocoagulation, coagulation, photo catalysis, cation-exchange membrane, chemical reduction, electroplating, oxidation, filtration, coagulation, precipitation, ion exchanging, reverse osmosis, flocculation, and adsorption are few methods that have been used to remove MB dye from aqueous solution [2-7].

Adsorption is often regarded as one of the utmost useful methods for managing effluents having dye due to its uncomplicated design, lack of secondary impurity, inexpensive cost, efficiency, and ease of handling. Different adsorbents utilized in the adsorption method like hydrogel adsorbents that have received best attention in the adsorption method because they are biodegradable, selective, affordable, effective, inherently nontoxic, and ecologically acceptable. Chitosan, Alginate, *k*-carrageenan, and cellulose have attracted attention recently because of how well they work as water treatment materials and adsorption. Among these treatment techniques, adsorption has been recognized as a more favorable method owing to its simplicity, better removal efficiency [8-11]. Commonly, the application of normal and feasible adsorbents in the adsorption methods has gained great attention. One of the important techniques used to eliminate pollutant is adsorption, especially using eco-friendly absorbent. Hydrogel is also proven to be non-toxic and environmentally friendly Poor binding properties were overcome by preparing stable nanoparticles in the polymer, particularly hydrogel networks in which the nanoparticles were embedded. Hydrogel can also be used as part of an integrated controlled system to reduce the dosage increase in drug delivery [12-15].

In the work, acrylamide based graft poly (acrylic acid) hydrogel (AM-g-P(AC)) and its nanocomposite with CdS nanoparticles AM-g-P(AC)/CdS were produced by the free radical method utilized as an effective adsorbent for the adsorption of basic dye alike MB dye. The properties of structural hydrogel have been estimated *via* utilizing several analytical instrumentation techniques like FE-SEM, TEM, FT-IR, and XRD. The effect of equilibrium time, pH, adsorbent dose, and concentration of MB dye has been studied and also antibacterial activity has been analyzed. The adsorption efficiency has been estimation via the adsorption isotherm like isotherm Freundlich and isotherm Langmuir models.

Experimental

Materials and methods

Acrylamide (AM) and acrylic acid (AC) ware supplied by Sigma-Aldrich, Germany. The cross-linked *N,N'*-methylene bisacrylamide (MBA) was purchased from Fluka, Germany potassium persulfate (KPS) was supplied by Merck, Germany. Sodium chloride was obtained from Alpha Chemika and sodium hydroxide and hydrochloric acid were supplied from Sigma-Aldrich, Germany.

Preparation of stock solution for MB dye

A stock solution was created by dissolving 0.5 g of in 500 mL distilled water. MB dye, as shown in Figure 1, has molecular formula ($C_{16}H_{18}ClN_3S$) and molecular weight (319.85 g·mol^{-1}). MB dye is odorless blue powder. Its maximum wavelength was λ_{max} = 630 nm. The calibration curve was prepared for a different concentrations of dye (2-10 mg.L^{-1}). λ_{max} = 630 nm, as displayed in Figure 1.

Preparation AM-g-P(AC)/CdS hydrogel nanocomposite

AM-g-P(AC)/CdS was prepared with CdS (1 g) with stirring 60 min and 0.5 g in 5 mL distilled water acryl amide (AM) at 25 °C, and added 3 mL in 2 mL distilled water of acrylic acid (AC), formerly additional, 0.05 g MBA, 0.03 g KPS in 5 mL distilled water, processes happen in attendance of nitrogen gas to form free radicals at 75 °C for 5 h. The AM-g-P(AC)/CdS washed more than a few times and dried in an oven at 75 °C for 12 h.

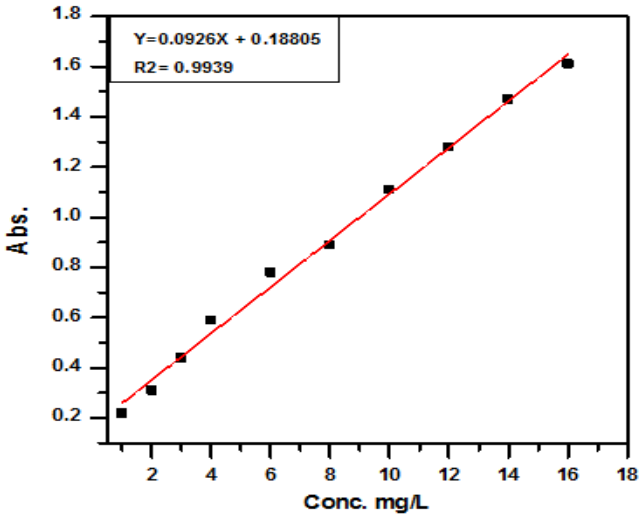

Figure 1. Calibration curve of MB dye

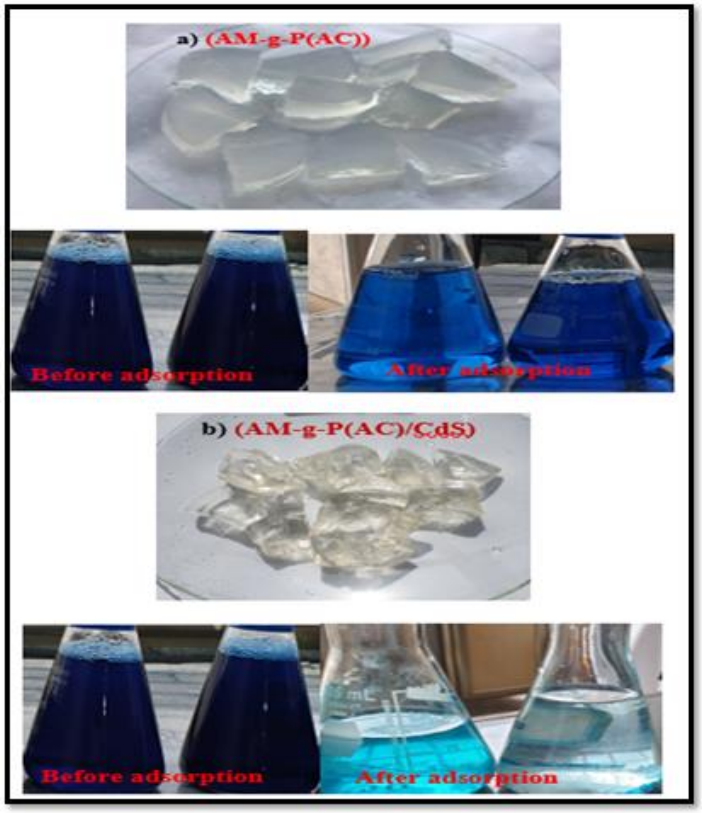

Figure 2. (a) shows image of AM-g-P(AC)/CdS with the way of elimination MB dye before and after adsorption and (b) shows image of AM-g-P(AC) with the process of removal MB dye before and after adsorption

It is worth to note that AM-g-P(AC) was prepared with the same steps as mentioned above without adding (CdS NPs). Figure 2a depicts image of the surface preparation AM-g-P(AC)/CdS with the way of elimination MB dye before and after loading dye. Figure 2b shows image of preparation AM-g-P(AC) with the way of elimination MB dye before, after loading dye.

Adsorption isotherm

All experiments were carried out under experimental conditions in a shaker water bath in 100 mL elementary flasks. The effect of several adsorption parameter, pH=3-10, initial concentration MB dye (100-500), and temperature solution (15-45 °C), were studied under the best adsorption experiment condition at 25 °C and rate agitation of 120 rpm. The residual concentration of MB dye in each aliquot was calculate via a UV-Vis spectrum. The adsorption efficiency (Qe) and removal efficiency (E%) adsorption were calculated in Equations 1 and 2.

$$\mathrm{Qe}\left(\frac{\mathrm{mg}}{\mathrm{g}}\right) = \frac{(\mathrm{Co} - \mathrm{Ce})\mathrm{Vml}}{\mathrm{M\,g}} \quad (1)$$

$$\mathrm{E\%} = \frac{\mathrm{Co} - \mathrm{Ce}}{\mathrm{Co}} \times 100 \quad (2)$$

Biochemical test of bacteria

Types of bacteria used (*Staphylococcus epidermidi* and *Staphylococcus aureus*) and (*E. coli* and *Klebsiella spp.)*, for this study were sourced from University of Babylon. Eosin methylene blue (EMB) and mannitol salt (MS)

agars were utilized for isolating, cultivating, and differentiating bacteria. In addition, the bacteria were identified using microscopic analysis, specifically Gram's staining method.

Antibacterial activity

The biological activity of the hydrogel nanocomposite before and after loading CdS to it was studied, as the study included the use of two types of pathogenic bacteria, positive for Sauries and negative for types of bacteria (10 mg/L), by drilling diffusion method to find out the inhibitory effect on growth these bacteria.

Results and Discussion

Characterization of nanocomposite

Also, the AM-g-P(AC)/CdS hydrogel nanocomposite was diagnosed before and after loading the (CdS) through the (FE-SEM), as shown in Figure 3a, the AM-g-P(AC)/CdS has a flat surface containing of layers compacted on each other as a result of due to the weak bond that binds the polymer layers together, in addition to due to the cross linking agent that showed a range wide of smoothness surface. In contrast, the CdS nanoparticles spread over the surface hydrogel, which enhances the ability of the AM-g-P(AC)/CdS to removal MB dye [16]. The nanocomposite after the adsorption process on to MB dye as show in Figure 3b, that it contains many irregular zigzags resulting from the filling of all the active sites, evidence of the efficiency of the surface and the successful occurrence of the adsorption process [17, 18].

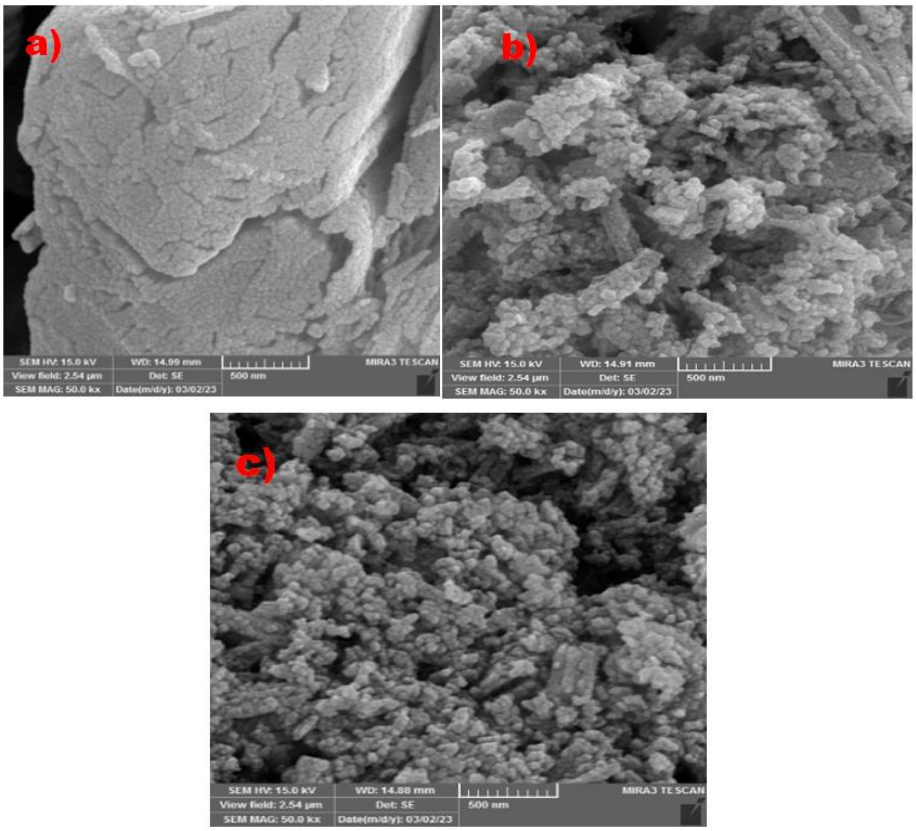

Figure 3. FE-SEM a) AM-g-P(AC) hydrogel, b) AM-g-P(AC)/CdS hydrogel nanocomposite, and c) hydrogel nanocomposite after adsorption MB dye

The TEM image showed the creation of new geometry after CdS NPs were decorated on the hydrogel surface; this can be attributed to the role of the amount of Cds NPs on the hydrogel surface. The geometric structure of the nanocomposite during their creation became clearer through TEM data. Figure 4 shows how the single-crystal plate structure takes the form of one cylinder stacked on top of another when CdS NPs are loaded. The results of TEM experiments showed that XRD and FESEM analyses were in good agreement [19, 20].

The AM-g-P(AC)/CdS hydrogel nanocomposite was diagnosed with FT-IR before adsorption and after loading dye, as depicted in Figure 5. Comparing the two shapes makes it noticeable that the beam is in about range 3350-3210 cm^{-1}. Over-lapping NH, and OH band because of bond hydrogen before adsorption proses, the decrease in intensity clearly happens due to after adsorption in Figure 5, which in turn leads to a decrease in the number of hydrogen bonds as well as the N-H bending beam shift from 1600 cm^{-1} to 1443 cm^{-1}, due to the presence of CdS in the compound, as well as a decrease in intensity, indicating the presence of CdS, as all this indicates that the CdS nanoparticles worked to decrease the ratio of the spectrum (decrease intensity) [21, 22].

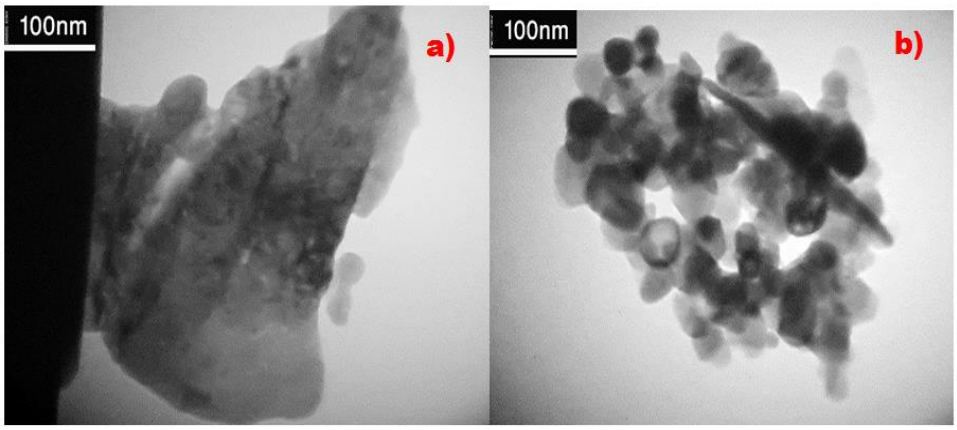

Figure 4. TEM a) AM-g-P(AC) hydrogel and b) AM-g-P(AC)/CdS hydrogel nanocomposite

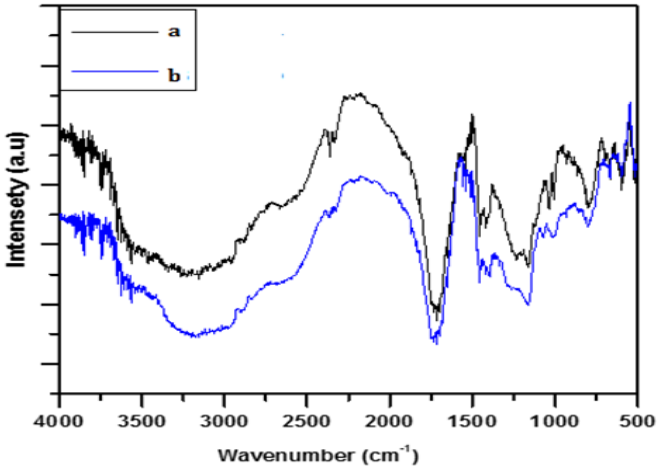

Figure 5. FT-IR of a) (AM-g-P(AC)/CdS) hydrogel nanocomposite before adsorption and b) nanocomposite after adsorption

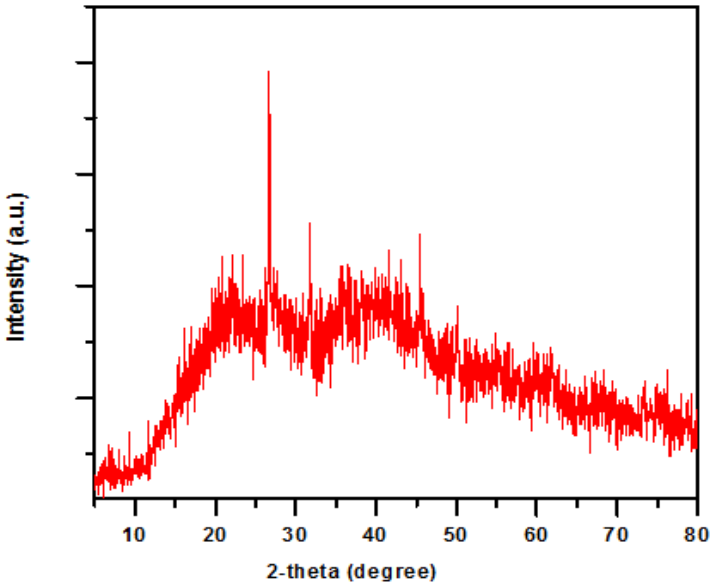

Figure 6. XRD of ((AM-g-P(AC)/CdS) hydrogel nanocomposite

Analysis of hydrogel nanocomposite loaded with CdS nanoparticles was done using X-ray diffraction by X-ray diffraction emitted from the Cu-Kα source with a wavelength of (1.5104 Ao) and an angular range of 2θ = 5-80. The broad peak in Figure 6 at 21.66°, 25.109°, and 38.13° indicates that the hydrogel composites are seam-crystalline [23, 24].

Effect of pH

The influence solution of pH on the adsorption process of MB dye on the surface of the adsorbent AM-g-P(AC)/CdS hydrogel nanocomposite was studied at a concentration of 300 mg/L at different values of the acid function within the range 3-10, and through the results demonstrated in Figure 7, it was noted that the amount of adsorption. The MB dye on the adsorbent surface increases with the increase in the acid function. That is, the adsorbent surface becomes negative, so the swelling rate increases, and this leads to increased dye adsorption. As a result, a repulsion process will occur for the negative charge between the negative groups on the hydrogel, which will cause swelling and expansion of the hydrogel, allowing the dye molecules to spread within the hydrogel, which will increase the adsorption process [25].

Effect of concentration of MB dye

The hydrogel nanocomposite was used to removal initial concentration of MB dye. The amount of adsorption required to remove initial concentration MB dye and the number of sites available on the adsorbent surface. The effect of removal concentration MB dye by hydrogel nanocomposite, Figure 8 displays the removal efficiency versus initial concentration of MB dye. The reduction in adsorption caused by a shortage of accessible active sites causes the drug clearance percentage to decline as concentration of MB dye rises. As drug uptake resistance reduces as MB dye concentration rises, the adsorption capacity ((Qe) mg/g) is proportional to initial dye concentration. Due to an increase in driving force, the adsorption rate likewise rises as the dye's starting concentration does [26, 27].

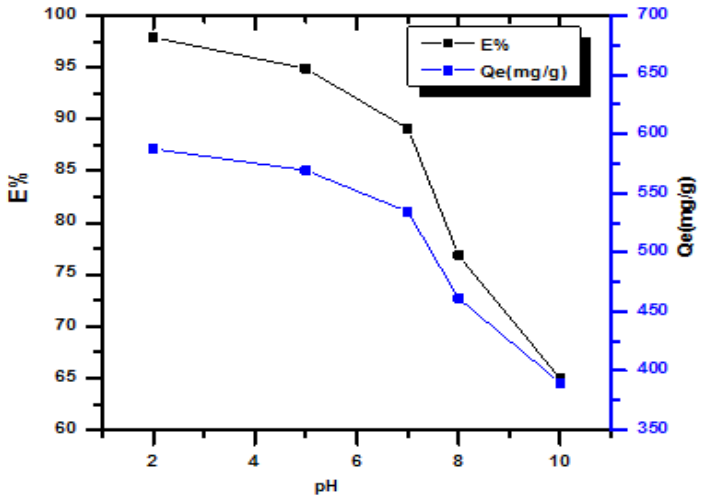

Figure 7. Effect of pH solution on to adsorption capacity and removal MB dye

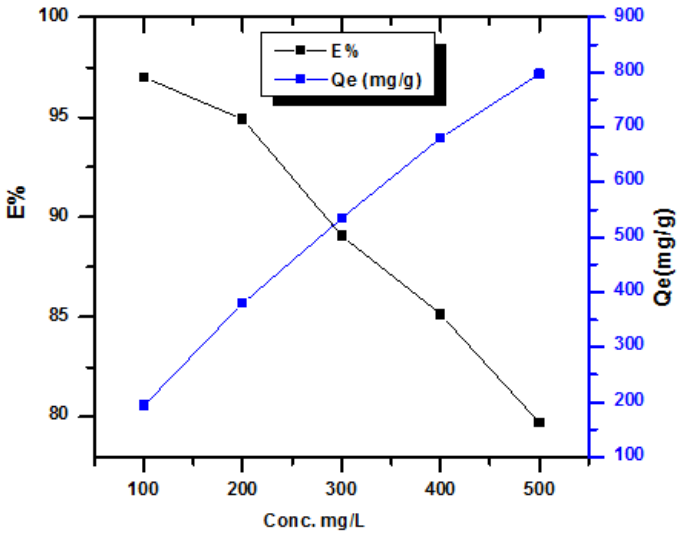

Figure 8. Effect on initial concentration on to removal percentage by using hydrogel nanocomposite

Effect of mass of hydrogels

Several quantities of the adsorbent surfaces AM-g-P(AC)/CdS and AM-g-P(AC) were tested to see how they affected the adsorption of the MB, which would indicate the ideal adsorbent mass. To do this, several quantities of AM-g-P(AC)/CdS and AM-g-P(AC) 0.01 - 0.12 g for 100 mg/L of MB dye solution [28]. The samples were shaken in shaker water bath for 120 min at 25 °C. To obtain a clear solution, use centrifuge for 10 minutes to separate the solution. Thus, the ideal weight for the adsorption process to remove MB dye from the aqueous solution was determined through the relationship between the adsorption efficiency and the removal efficiency versus the weight of the hydrogel. When increase adsorbent dosage increase removal percentage (E%) of 82% to 99.9%, 67% to 89% but decrease adsorption capacity 231.45-2423.45 mg/g, 215.11-2054.45 mg/g for AM-g-P(AC)/CdS and AM-g-P(AC) of MB dye has been attained, as shown in Figures 9 and 10 [29, 30].

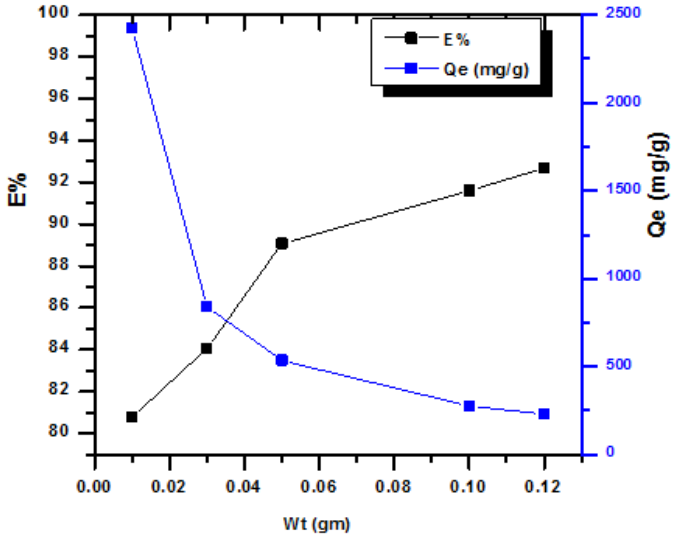

Figure 9. Effect of adsorption dosage of AM-g-P(AC)/CdS hydrogel nanocomposite on to removal MB dye

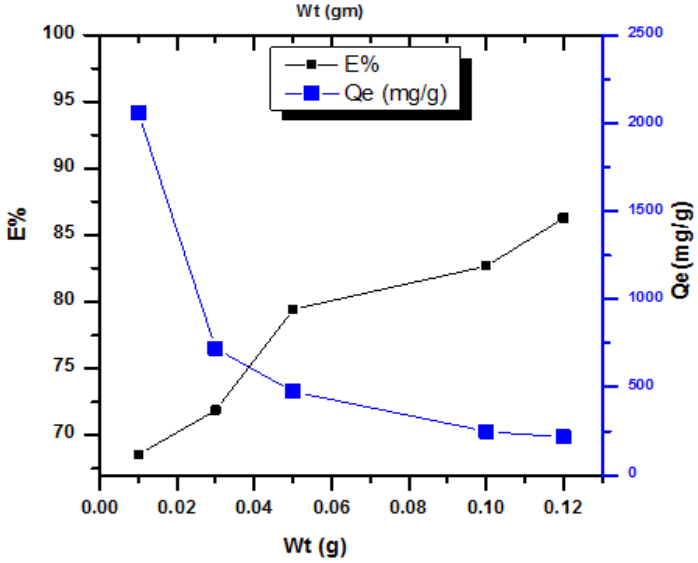

Figure 10. Effect of adsorption dosage of AM-g-P(AC) hydrogel on to removal MB dye

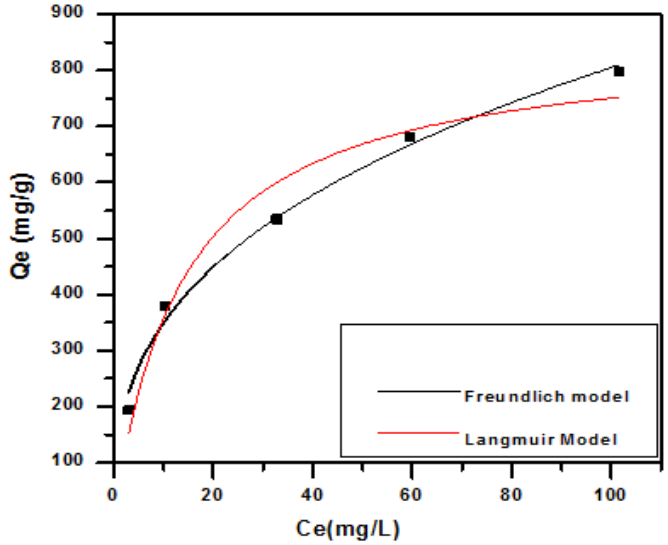

Figure 11. Non-linear fit of adsorption isotherm non-liner models of MB on nanocomposite

Adsorption isotherm study

In adsorption equilibrium studies, two isotherm models are utilized, notably Langmuir and Freundlich, models were calculated by Equations 3 and 4.

$$q_e = \frac{q_m K_L C_e}{1 + K_L C_e} \quad (3)$$

$$q_e = \frac{q_m K_L C_e}{1 + K_L C_e} \quad (4)$$

Where, q_e: amount adsorbed per unit weight of the adsorbent at equilibrium (mg/g), (mol/g), Ce: equilibrium concentration of the adsorbate in solution following adsorption (mg/L), (mol/L), Kf: empirical Freundlich constant or capacity factor (L/g), q_m: maximum adsorption capacity (mg/g), and K_L: Langmuir constant (L/mg). The Langmuir isotherm, as demonstrated in Figure 11, assumes a finite number of uniform active sites on the adsorbent surface, leading to the formation of a monomolecular layer with minimal intermolecular interactions. In contrast, the Freundlich isotherm, also presented in Figure 6, is applicable to heterogeneous surface adsorption. It implies a direct proportionality between adsorbate concentration and adsorbent quantity on the surface, coupled with a decrease in sorption energy upon saturation of the adsorbent's sorption centers [31, 32]. To assess the dye-nanocomposite system, the coefficient of determination (R^2) was computed by fitting the experimental data to these isotherms Figure 11 and Table 1 illustrate that the Langmuir isotherm provides a more robust correlation, evidenced by the highest R^2 value of 0.93833 [33, 34].

Antibacterial activity

The biological compound activity results were observed before and after the process of loading CdS NPs on it against the types of bacteria used *Staphylococcus epidermidi*, *Staphylococcus aureus*, *E. coli*, and *Klebsiella spp.*, as illustrated in Figure 12, AM-g-P(AC)/CdS hydrogel nanocomposite shows high effectiveness against positive and negative bacteria.

Table 1. Different parameter adsorption isotherm model of MB dye onto nanocomposite

Freundlich	K_f	151.77	15.667
	1/n	0.362	0.0225
	R^2	0.9898	
Langmuir	q_m (mg/g)	854.57	68.385
	K_L (L/mg)	0.0718	0.0212
	R^2	0.9499	

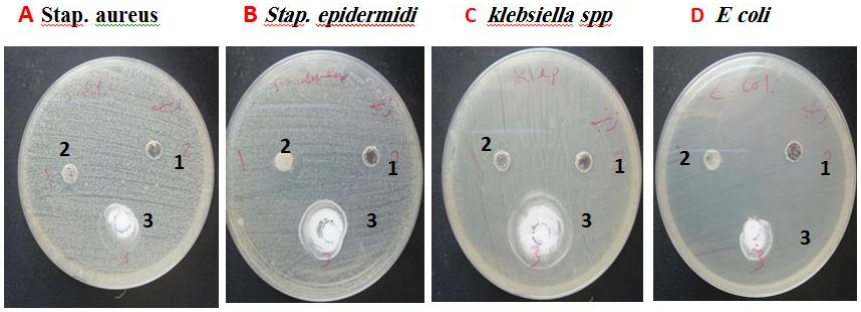

Figure 12. Anti-bacterial activities of the (1) Control, (2) AM-g-P(AC) hydrogel, and (3) AM-g-P(AC)/CdS hydrogel nanocomposite utilizing disc diffusion method

As for the other prepared concentrations, AM-g-P(AC) hydrogel they showed their effectiveness in varying degrees, compares with control, as shown in Figure 12.

Conclusion

The adsorption effectiveness of the AM-g-P(AC)/CdS hydrogel nanocomposite surface highlights the successful incorporation of CdS nanoparticles. High concentrations of CdS NPs on the surface signify its enhanced efficacy. Our findings indicate that the removal of MB by the hydrogel increases with decreasing pH, with optimal removal observed at pH=2. This phenomenon can be attributed to repulsion forces among negatively charged functional groups on the adsorbent surface, facilitating swelling and increased dye adsorption within the hydrogel matrix. Furthermore, determining the ideal mass for MB adsorption can be achieved by plotting the removal percentage (E%) against the mass of the hydrogel. Increasing the adsorbent dosage significantly enhances removal efficiency, ranging from 82% to 99.9% for AM-g-P(AC)/CdS and 67% to 89% for AM-g-P(AC), albeit with a reduction in adsorption capacity from 215.11 mg/g to 2054.45 mg/g.

Disclosure Statement

No potential conflict of interest was reported by the authors.

Funding

This study was funded by Payame Noor University (PNU) Research Council.

Authors' Contributions

All authors contributed to data analysis, drafting, and revising of the article and agreed to be responsible for all the aspects of this work.

Orcid

Aseel M. Aljeboree
https://orcid.org/0000-0002-0853-6075
Ola Hamad Salah
https://orcid.org/0000-0002-3194-1749
Manal Morad Karim
https://orcid.org/0000-0003-0061-0389
Salima B. Alsaadi
https://orcid.org/0009-0004-3760-4489
Mohammed Abed Jawad
https://orcid.org/0009-0002-7479-3333
Ayad F. alkaim
https://orcid.org/0000-0003-3459-4583

References

[1]. Esfandiyari T., Nasirizadeh N., Ehrampoosh M.H., Tabatabaee M. Characterization and absorption studies of cationic dye on multi walled carbon nanotube–carbon ceramic composite. *Journal of Industrial and Engineering Chemistry*, 2017, **46**:35 [Crossref], [Google Scholar], [Publisher]

[2]. Allah M.A.A.H., Alshamsi H.A. Green synthesis of AC/ZnO nanocomposites for adsorptive removal of organic dyes from aqueous solution. *Inorganic Chemistry Communications*, 2023, **157**:111415 [Crossref], [Google Scholar], [Publisher]

[3]. Saxena M., Sharma N., Saxena R. Highly efficient and rapid removal of a toxic dye: adsorption kinetics, isotherm, and mechanism studies on functionalized multiwalled carbon nanotubes. *Surfaces and Interfaces*, 2020, **21**:100639 [Crossref], [Google Scholar], [Publisher]

[4]. Azha S.F., Nasir N.N.M., Musa J., Ismail S. Binary adsorption of textile dyes onto zwitterionic adsorbent coating: Performance study. *Current Research in Wastewater Management*, 2021, **1**:23 [Crossref], [Google Scholar], [Publisher]

[5]. a) Nakhjiri M.T., Marandi G.B., Kurdtabar M. Poly (AA-co-VPA) hydrogel cross-linked with N-maleyl chitosan as dye adsorbent: Isotherms,

kinetics and thermodynamic investigation. *International Journal of Biological Macromolecules*, 2018, **117**:152 [Crossref], [Google Scholar], [Publisher]; b) Zamani, A., Asghari S., Tajbakhsh M. Synthesis of TiO_2/CD and TiO_2/Ag/CD nanocomposites and investigation of their visible light photocatalytic activities in the degradation of methylene blue. *Chemical Methodologies*, 2024, **8**:177 [Crossref], [Publisher]

[6]. a) Magriotis Z.M., Carvalho M.Z., de Sales P.F., Alves F.C., Resende R.F., Saczk A.A.. Castor bean (Ricinus communis L.) presscake from biodiesel production: An efficient low cost adsorbent for removal of textile dyes. *Journal of Environmental Chemical Engineering*, 2014, **2**:1731 [Crossref], [Google Scholar], [Publisher]; b) Dourandish Z., Garkani Nejad F., Zaimbashi R., Tajik S., Askari M.B., Salarizadeh P., Mohammadi S.Z., Oloumi H., Mousazadeh F., Baghayeri M., Beitollai H. Recent advances in electrochemical sensing of anticancer drug doxorubicin: A mini-review. *Chemical Methodologies*, 2024, **8**:293 [Crossref], [Publisher]; c) Abegunde S.M., Idowu K. S. Enhanced adsorption of methylene blue dye from water by alkali-treated activated carbon. *Eurasian Journal of Science and Technology*, 2023, **3**:109 [Crossref], [Publisher]

[7]. a) Chen L., Zhu Y., Cui Y., Dai R., Shan Z., Chen H. Fabrication of starch-based high-performance adsorptive hydrogels using a novel effective pretreatment and adsorption for cationic methylene blue dye: Behavior and mechanism. *Chemical Engineering Journal*, 2021, **405**:126953 [Crossref], [Google Scholar], [Publisher]; b) Alizadeh K., Khaledyan E., Mansourpanah Y. Novel modified magnetic mesopouros silica for rapid and efficient removal of methylene blue dye from aqueous media. *Journal of Applied Organometallic Chemistry*, 2022, **2**:198 [Crossref], [Publisher]

[8]. Aljeboree A., Essa S., Kadam Z., Dawood F., Falah D., AF A. Environmentally friendly activated carbon derived from palm leaf for the removal of toxic reactive green dye. *International Journal of Pharmaceutical Quality Assurance*, 2023, **14**:12 [Crossref], [Google Scholar], [Publisher]

[9]. Saxena M., Lochab A., Saxena R. Asparagine functionalized MWCNTs for adsorptive removal of hazardous cationic dyes: Exploring kinetics, isotherm and mechanism. *Surfaces and Interfaces*, 2021, **25**:101187 [Crossref], [Google Scholar], [Publisher]

[10]. Salman M.S., Sheikh M.C., Hasan M.M., Hasan M.N., Kubra K.T., Rehan A.I., Awual M.E., Rasee A.I., Waliullah R., Hossain M.S. Chitosan-coated cotton fiber composite for efficient toxic dye encapsulation from aqueous media. *Applied Surface Science*, 2023, **622**:157008 [Crossref], [Google Scholar], [Publisher]

[11]. Zhu L., Guan C., Zhou B., Zhang Z., Yang R., Tang Y., Yang J. Adsorption of dyes onto sodium alginate graft poly (acrylic acid-co-2-acrylamide-2-methyl propane sulfonic acid)/kaolin hydrogel composite, *Polymers and Polymer Composites*, 2017, **25**:627 [Crossref], [Google Scholar], [Publisher]

[12]. Liu Y., Chen Y., Shi Y., Wan D., Chen J., Xiao S. Adsorption of toxic dye Eosin Y from aqueous solution by clay/carbon composite derived from spent bleaching earth. *Water Environment Research*, 2021, **93**:159 [Crossref], [Google Scholar], [Publisher]

[13]. Radjai M., Ferkous H., Jebali Z., Majdoub H., Bourzami R., Raffin G., Achour M., Gil A., Boutahala M. Adsorptive removal of cationic and anionic dyes on a novel mesoporous adsorbent prepared from diatomite and anionic cellulose nanofibrils: Experimental and theoretical investigations. *Journal of Molecular Liquids*, 2022, **361**:119670 [Crossref], [Google Scholar], [Publisher]

[14]. Mandal B., Ray S.K. Removal of safranine T and brilliant cresyl blue dyes from water by carboxy methyl cellulose incorporated acrylic hydrogels: Isotherms, kinetics and thermodynamic study. *Journal of the Taiwan Institute of Chemical Engineers*, 2016, **60**:313 [Crossref], [Google Scholar], [Publisher]
[15]. Abd Malek N.N., Jawad A.H., Ismail K., Razuan R., ALOthman Z.A. Fly ash modified magnetic chitosan-polyvinyl alcohol blend for reactive orange 16 dye removal: Adsorption parametric optimization. *International Journal of Biological Macromolecules*, 2021, **189**:464 [Crossref], [Google Scholar], [Publisher]
[16]. Radia N., Kamona S., Jasem H., Abass R., Izzat S., Ali M., Ghafel S., Aljeboree A. Role of hydrogel and study of its high-efficiency to removal streptomycin drug from aqueous solutions. *International Journal of Pharmaceutical Quality Assurance*, 2022, **13**:160 [Google Scholar]
[17]. Thakur S., Chaudhary J., Thakur A., Gunduz O., Alsanie W.F., Makatsoris C., Thakur V.K. Highly efficient poly (acrylic acid-co-aniline) grafted itaconic acid hydrogel: Application in water retention and adsorption of rhodamine B dye for a sustainable environment. *Chemosphere*, 2022, **303**:134917 [Crossref], [Google Scholar], [Publisher]
[18]. Alhattab Z.D., Aljeboree A.M., Jawad M.A., Sheri F.S., Obaid Aldulaim A.K., Alkaim A.F. Highly adsorption of alginate/bentonite impregnated TiO2 beads for wastewater treatment: Optimization, kinetics, and regeneration studies. *Caspian Journal of Environmental Sciences*, 2023, **21**:657 [Crossref], [Google Scholar], [Publisher]
[19]. Sharma S., Sharma G., Kumar A., AlGarni T.S., Naushad M., ALOthman Z.A., Stadler F.J. Adsorption of cationic dyes onto carrageenan and itaconic acid-based superabsorbent hydrogel: Synthesis, characterization and isotherm analysis. *Journal of Hazardous Materials*, 2022, **421**:126729 [Crossref], [Google Scholar], [Publisher]
[20]. Shirsath S., Patil A., Bhanvase B., Sonawane S. Ultrasonically prepared poly (acrylamide)-kaolin composite hydrogel for removal of crystal violet dye from wastewater. *Journal of Environmental Chemical Engineering*, 2015, **3**:1152 [Crossref], [Google Scholar], [Publisher]
[21]. Shen Y., Li B., Zhang Z. Super-efficient removal and adsorption mechanism of anionic dyes from water by magnetic amino acid-functionalized diatomite/yttrium alginate hybrid beads as an eco-friendly composite. *Chemosphere*, 2023, **336**:139233 [Crossref], [Google Scholar], [Publisher]
[22]. Sharma S., Sharma G., Kumar A., AlGarni T.S., Naushad M., ALOthman Z.A., Stadler F.J. Adsorption of cationic dyes onto carrageenan and itaconic acid-based superabsorbent hydrogel: Synthesis, characterization and isotherm analysis. *Journal of Hazardous Materials*, 2022, **421**:126729 [Crossref], [Google Scholar], [Publisher]
[23]. Pashaei-Fakhri S., Peighambardoust S.J., Foroutan R., Arsalani N., Ramavandi B., Crystal violet dye sorption over acrylamide/graphene oxide bonded sodium alginate nanocomposite hydrogel. *Chemosphere*, 2021, **270**:129419 [Crossref], [Google Scholar], [Publisher]
[24]. Samiyammal P., Kokila A., Pragasan L.A., Rajagopal R., Sathya R., Ragupathy S., Krishnakumar M., Reddy V.R.M. Adsorption of brilliant green dye onto activated carbon prepared from cashew nut shell by KOH activation: Studies on equilibrium isotherm. *Environmental Research*, 2022, **212**:113497 [Crossref], [Google Scholar], [Publisher]
[25]. Zhao Y., Chen Y., Zhao J., Tong Z., Jin S. Preparation of SA-g-(PAA-co-PDMC) polyampholytic superabsorbent polymer and its application to the anionic dye adsorption removal from effluents. *Separation and*

Purification Technology, 2017, **188**:329 [Crossref], [Google Scholar], [Publisher]

[26]. Zhao Y., Li B. Preparation and superstrong adsorption of a novel La (Ⅲ)-crosslinked alginate/modified diatomite macroparticle composite for anionic dyes removal from aqueous solutions. *Gels*, 2022, **8**:810 [Crossref], [Google Scholar], [Publisher]

[27]. Al-Mashhadani Z., Aljeboree A., Radia N., Alkadir O. Antibiotics Removal by adsorption onto eco-friendly surface: characterization and kinetic study. *International Journal of Pharmaceutical Quality Assurance*, 2021, **12**:252 [Google Scholar]

[28]. Taifi A., Alkadir O.K.A., Aljeboree A.M., Al Bayaa A.L., Alkaim A.F., Abed S.A. Environmental removal of reactive blue 49 dye from aqueous solution by (Lemon peels as activated carbon): A model of low cost agricultural waste. *IOP Conference Series: Earth and Environmental Science*, 2022, 012010 [Google Scholar], [Publisher]

[29]. Soury R., Jabli M., Latif S., Alenezi K.M., El Oudi M., Abdulaziz F., Teka S., El Moll H., Haque A. Synthesis and characterization of a new meso-tetrakis (2, 4, 6-trimethylphenyl) porphyrinto) zinc (II) supported sodium alginate gel beads for improved adsorption of methylene blue dye. *International journal of Biological Macromolecules*, 2022, **202**:161 [Crossref], [Google Scholar], [Publisher]

[30]. Radia N.D., Mahdi A.B., Mohammed G.A., Sajid A., Altimari U.S., Shams M.A., Aljeboree A.M., Fh A. Removal of rose bengal dye from aqueous solution using low cost (sa-g-paac) hydrogel: equilibrium and kinetic study. *International Journal of Drug Delivery Technology*, 2022, **12**:957 [Google Scholar], [Publisher]

[31]. Aljeboree A.M., Alhattab Z.D., Altimari U.S., Aldulaim A.K.O., Mahdi A.K., Alkaim A.F. Enhanced removal of amoxicillin and chlorophenol as a model of wastewater pollutants using hydrogel nanocomposite: Optimization, thermodynamic, and isotherm studies. *Caspian Journal of Environmental Sciences*, 2023, **21**:411 [Crossref], [Google Scholar], [Publisher]

[32]. Thakur S., Chaudhary J., Thakur A., Gunduz O., Alsanie W.F., Makatsoris C., Thakur V.K. Highly efficient poly (acrylic acid-co-aniline) grafted itaconic acid hydrogel: Application in water retention and adsorption of rhodamine B dye for a sustainable environment. *Chemosphere*, 2022, **303**:134917 [Crossref], [Google Scholar], [Publisher]

[33]. Vieira T., Artifon S.E., Cesco C.T., Vilela P.B., Becegato V.A., Paulino A.T. Chitosan-based hydrogels for the sorption of metals and dyes in water: isothermal, kinetic, and thermodynamic evaluations. *Colloid and Polymer Science*, 2021, **299**:649 [Crossref], [Google Scholar], [Publisher]

[34]. Ilgin P., Ozay H., Ozay O. Selective adsorption of cationic dyes from colored noxious effluent using a novel N-tert-butylmaleamic acid based hydrogels. *Reactive and Functional Polymers*, 2019, **142**:189 [Crossref], [Google Scholar], [Publisher]

How to cite this manuscript: Aseel M. Aljeboree, Ola Hamad Salah, Manal Morad Karim, Salima B. Alsaadi, Mohammed Abed Jawad, Ayad F. Alkaim. Synthesis and Characterization of Acrylamide-based Graft Poly(acrylic acid) Hydrogel Nanocomposite for Methylene Blue Dye Removal and Investigation Isotherm Models. *Asian Journal of Green Chemistry*, 8(4) 2024, 382-396.
DOI: 10.48309/AJGC.2024.455843.1501